Vibration Suppression Control for an Articulated Robot: Effects of Model-Based Control Integrated into the Position Control Loop

Masahiko ITOH*

* Department of Mechanical Engineering, Miyagi National College of Technology, Natori-shi, Japan
(Tel : +81-22-381-0316; E-mail: itoh@miyagi-ct.ac.jp)

Abstract: This paper deals with a control technique of eliminating the transient vibration with respect to a waist axis of an articulated robot. This control technique is based on a model-based control in order to establish the damping effect on the driven mechanical part. The control model is composed of reduced-order electrical and mechanical parts related to the velocity control loop. The parameters of the control model can be obtained from design data or experimental data. This model estimates a load speed converted to the motor shaft. The difference between the estimated load speed and the motor speed is calculated dynamically, and it is added to the velocity command to suppress the transient vibration. This control method is applied to an articulated robot regarded as a time-invariant system. The effectiveness of the model-based control integrated into the position control loop is verified by simulations. Simulations show satisfactory control results to reduce the transient vibration at the end-effector.

Keywords: Articulated Robot, Geared System, Waist Axis of Robot, Vibration Control, Damping, Model-Based Control, Reduced-Order Model, Position Control Loop.

1. INTRODUCTION

Most of the industrial robots have the geared reduction mechanisms between output shafts of motors and driven machine parts. For instance, spur gears, harmonic drive gear reducers, RV gear reducers and so on are well known. As industrial applications, higher speed and higher accuracy operations are required for the industrial robots in recent years.The insufficiency of the torsional stiffness of the geared reduction mechanism often induces transient vibrations mainly related to the eigenvalues of the mechanical parts in the lower-frequency range when the motor starts or stops. This transient vibration causes a problem such that the tact time of the system may be lengthened and the tracking accuracy may be deteriorated.

To solve this problem, the full-closed loop control which feeds back the state variables measured with sensors at the end-effectors [1], the state-feedback control using observers [2][3], the velocity feedback control with a disturbance observer [4] and the dynamic damper comprised of the software [5] have been proposed.

However, the full-closed loop control technique and the control technique using an additional sensor are hard to set up in reality and incur increasing the cost. Further, the conventional observer technique to suppress the transient vibration requires a precise model of the mechanical system and an additional low-pass filter in a compensating loop. As a result, the observer technique has difficulties in setting up and adjusting its parameters in the field.

On the other hand, the author had proposed a simple and easily realizable technique for eliminating the transient vibration of a geared mechanical system [6]. This technique is based on a model-based control. The control model is related to the velocity control loop, and it is composed of reduced-order electrical and mechanical parts by considering that the transient vibration which should be eliminated is mainly dominated by the first mode of vibration in the geared mechanical system. This model calculates the rotational speed of the driven mechanical part, which is converted to the motor shaft. The difference between the calculated rotational speed of the driven machine part and the motor speed is calculated dynamically, and it is added to the velocity command to suppress the transient vibration of the end-effector after being multiplied by a gain. The function of this technique is to establish a damping effect at the driven mechanical part. In referring to the construction, this model-based control loop as a dynamical compensator can be integrated into the position control loop as an inner loop. The control model is easily obtained from design or experimental data. Its algorithm can be easily installed into a DSP. Further, parameters of the control model are easily adjusted in the field.

In [7], this control technique was applied to a waist axis of a robot system which was composed of a motor, a harmonic drive gear reducer and a robot arm with 5 degrees of freedom, regarded as a time-invariant system. The settling times of the residual vibrations of 7 Hz and 12 Hz could be shortened down to about 1/2 of the uncompensated vibration level.

In addition, in [8], simulations and experiments on the time responses verified the effectiveness of the model-based control technique using a time-varying control model. The settling time of the residual vibration of 7 Hz or 12 Hz, which depends on the arm posture, could be shortened down to about 1/2 of the uncompensated vibration level.

In this paper, the effectiveness of the model-based control integrated into the position control loop is verified by simulations. Here, an articulated robot is regarded as a time-invariant system. Simulations on the time responses show satisfactory control results in reducing the transient vibration of 7 Hz or 12 Hz. As a result, the transient vibrations in the stating and the arrival phases of the operation can be suppressed.

2. REDUCED-ORDER MODEL OF AN ARTICULATED ROBOT SYSTEM

2.1 Equations of motion

As a typical example of the robot system, an articulated robot shown in Fig.1 (a) is taken up. A harmonic drive gear reducer whose reduction ratio is 1/100 is connected to a motor, and a driven machine part is connected to this reducer's output shaft. This system can be regarded as a 3-mass system composed of a motor rotor, a gear reducer's input shaft and a driven machine part as shown in Fig.1 (b), and it is controlled by the velocity control loop using the PI control.

Equations of motion of this geared system are written as

$$\begin{aligned} &J_m\ddot{\theta}_m + C_s(\dot{\theta}_m - \dot{\theta}_g) + K_s(\theta_m - \theta_g) = T_m, \\ &J_g\ddot{\theta}_g + C_s(\dot{\theta}_g - \dot{\theta}_m) + K_s(\theta_g - \theta_m) \\ &\quad + \{C_g(\dot{\theta}_g / R_g - \dot{\theta}_l) + K_g(\theta_g / R_g - \theta_l)\} / R_g = 0, \\ &J_l\ddot{\theta}_l + C_g(\dot{\theta}_l - \dot{\theta}_g / R_g) + K_g(\theta_l - \theta_g / R_g) = 0, \end{aligned} \tag{1}$$

where

θ_m = angular rotation of the motor,
θ_g = angular rotation of the gear reducer's input shaft,
θ_l = angular rotation of the driven machine part,
T_m = output torque of the motor,
J_m = moment of inertia of the motor rotor,
J_g = moment of inertia of the reducer's input shaft,
J_l = moment of inertia of the driven machine part,
R_g = reduction ratio of the gear reducer,
K_s = torsional stiffness between the motor rotor and the gear reducer's input shaft,
K_g = torsional stiffness of the gear reducer,
C_s = damping factor between the motor rotor and the gear reducer's input shaft,
C_g = damping factor of the gear reducer.

Further, when the motor speed is controlled by the PI control, equations related to the motor armature are expressed as

$$L\frac{di}{dt} = K_c(K_v e + \frac{K_v}{T_i}\int e dt - K_{cb} i) - Ri - K_e\omega_m, \tag{2}$$

$$e = \omega_{cmd} - \omega_m.$$

The output torque of the motor is expressed as

$$T_m = K_t i \tag{3}$$

where

ω_{cmd} = velocity command,
ω_m = rotating speed of the motor,
ω_g = rotating speed of the gear reducer's input shaft (= rotating speed of the wave generator),
ω_l = rotating speed of the driven machine part,
e =error,
i = current of the armature,
R = motor armature resistance,
L = motor armature inductance,
K_t = torque constant,
K_e = voltage constant,
K_c = current loop gain,
K_{cb} = current feedback gain,
K_v = proportional gain of the PI control,
T_i = integral time constant of the PI control.

According to Eqs.(1)~(3), a block diagram of the waist axis of the robot arm can be expressed as Fig.2.

2.2 Reduced-order model of mechanical part

This paper deals with a case such that the residual vibration is mainly dominated by the first vibration mode and the higher order vibration modes are apart from the first one. As a result, the 3-mass system shown in Fig.2 is transformed into a 2-mass system shown in Fig.3 by considering only the first vibration mode. In this reduced-order model, the natural angular frequency ω_n and the damping ratio γ_n are expressed as

$$\begin{aligned} \omega_n &= \sqrt{K_g{}^m(1/J_m{}^m + 1/J_l{}^m)}, \\ \gamma_n &= \frac{C_g{}^m(1/J_m{}^m + 1/J_l{}^m)}{2\omega_n}, \end{aligned} \tag{4}$$

where

$$\begin{aligned} J_m^m &= J_m + J_g, \\ J_l^m &= J_l / R_g^2, \\ K_g^m &= K_g / R_g^2, \\ C_g^m &= C_g / R_g^2. \end{aligned} \tag{5}$$

Here, the superscript "m" shows that parameters belong to the model. Defining the inertia ratio R_n as $R_n = J_l^m / J_m^m$ and transforming Eq.(4), J_l^m, K_g^m and C_g^m are expressed as

$$\begin{aligned} J_l^m &= R_n J_m^m, \\ K_g^m &= \frac{R_n J_m^m}{1 + R_n}\omega_n^2, \\ C_g^m &= \frac{2R_n J_m^m}{1 + R_n}\gamma_n\omega_n. \end{aligned} \tag{6}$$

Using this expression, the reduced order model can be easily obtained from not only design data but also measured data.

2.3 Reduced-order model of electrical part

Next, a reduced order electrical model can be obtained. Here, the effect of the counter electromotive force is ignored. Further, considering that the angular cut-off frequency ω_c of the current control loop is much higher than the first natural angular frequency of the mechanical system and the current loop gain within ω_c is about 1.0, the current control system composed of the current control loop and the torque constant is expressed as a proportional gain K_t^m. As a result, a simplified PI control system is obtained as shown in Fig.3.

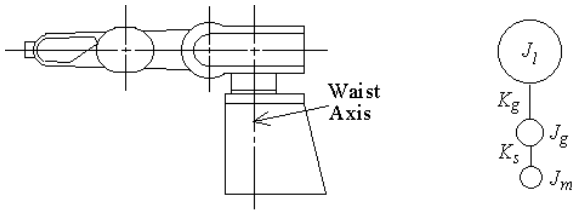

(a) Robot arm. (b) Model.

Fig. 1. A robot arm and its analytical model.

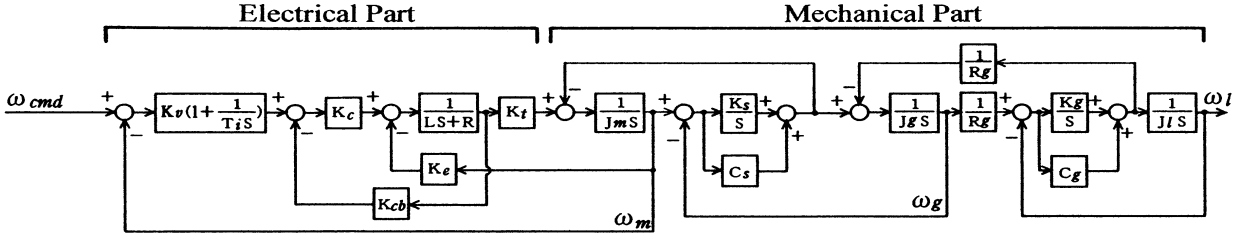

Fig. 2. Block diagram of a waist axis of an articulated robot.

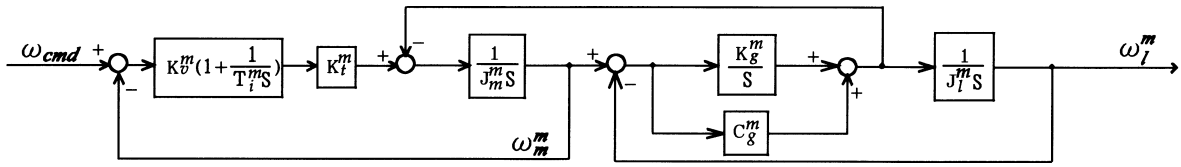

Fig. 3. Block diagram of reduced-order system.

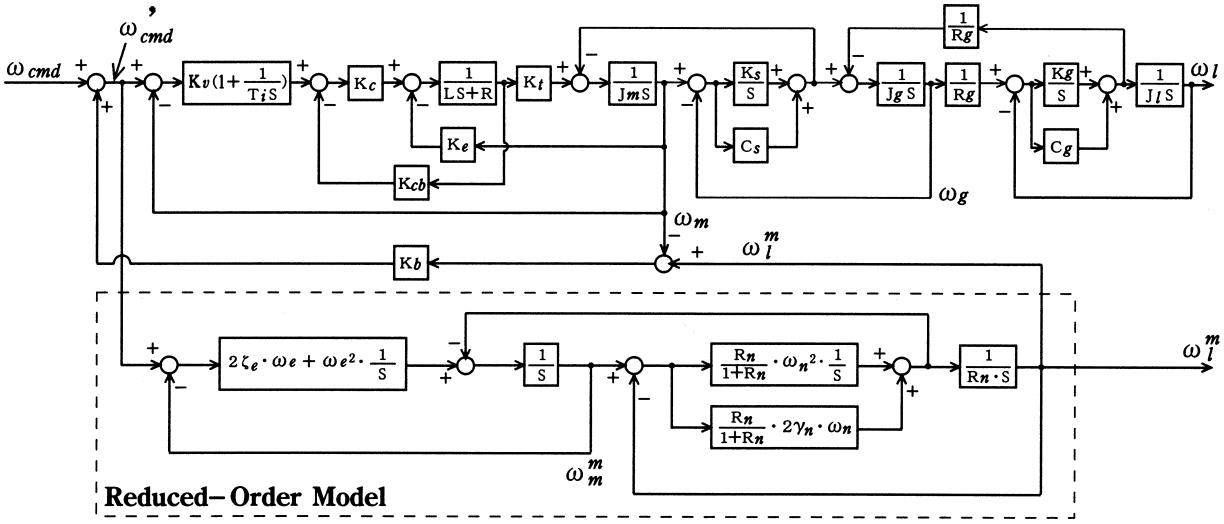

Fig. 4. Block diagram of model-based control.

Expressing the natural angular frequency ω_e and the damping ratio ζ_e of the electrical part as Eq. (7), the parameters of the reduced-order model can be easily adjusted.

$$\omega_e = \sqrt{\frac{K_v{}^m K_t{}^m}{T_i{}^m J_m{}^m}}, \qquad \zeta_e = \frac{1}{2}\sqrt{\frac{T_i{}^m K_v{}^m K_t{}^m}{J_m{}^m}}, \tag{7}$$

where $K_v^m = K_v$ and $T_i^m = T_i$.

3. CONSTRUCTION OF MODEL-BASED CONTROL SYSTEM [7]

3.1 Control System

Fig.4 shows a block diagram of the model-based control system related to the velocity control loop. Using the relationship of Eqs.(4)~(7), the block diagram of the reduced-order model shown in Fig.3 is transformed into the dotted-line part in Fig. 4.

When the moment of inertia of the driven machine part J_l with respect to the waist axis varies depending on the arm posture change, the model-based control can be applied with setting the parameters R_n, ω_n and γ_n to follow the values of the real system according to Eqs. (4)~(6).

In the compensating control system, the difference between the load's speed $\omega_l{}^m$ which is estimated at the motor shaft and the motor speed ω_m is dynamically calculated, and it is multiplied by the gain K_b. Finally, $K_b(\omega_l{}^m - \omega_m)$ is added to the velocity command ω_{cmd} as follows:

$$\omega'_{cmd} = \omega_{cmd} + K_b(\omega_l{}^m - \omega_m). \tag{8}$$

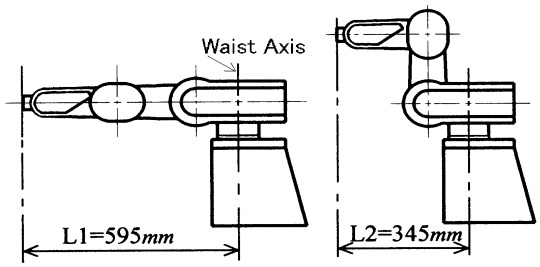

(a)Posture1 (N.F.=7Hz). (b)Posture2 (N.F.=12Hz).

Fig. 5. Correlation of natural frequency with the posture.

3.2 Stability

Table 1 shows conditions for simulations. The first natural frequency of the mechanical system varies from 7 Hz to12 Hz depending on the arm posture as shown in Fig.5. In Fig.5, N.F. is shortened form of Natural Frequency. L1 and L2 respectively represent the rotating radius of the end-effector with respect to the waist axis for Posture1 and Posture2.

In the simulations, the stability is considered by calculating the loci of system eigenvalues when the value of K_b is changed from 0.0 to −1.0. To obtain the system eigenvalues, first the model-based control system shown in Fig.4 is re-expressed using the state variable approach, and then the eigenvalues of the system matrix are calculated.

Fig.6 shows the loci of system eigenvalues. In this Figure, eigenvalues of −11±47j and −16±73j are related to the first natural frequency of the torsional vibration for Posture1 and Posture2, respectively. Fig.6 indicates that the control system is stable on the condition of $-0.9 \le K_b \le 0.0$.

3.3 Simulation of time response

Here, with respect to Posture1, the time response is calculated by the Runge-Kutta method in order to verify the suppression effect on the residual vibration. Fig.7 shows simulation results. In these figures, *Arm accel.* represents the vibration acceleration in the direction of rotation at the point of L1 in Fig.5. In these simulations, a trapezoidal velocity profile is assigned. The constant acceleration in the start phase is 1000min^{-1}/28ms. The cruise velocity is 2000 min^{-1}. The constant deceleration in the arrival phase is -1000min^{-1}/28ms. The value of K_b is set to −0.7 after considering the simulation results of the stability.

Fig.7 indicates that the proposed model-based control suppresses the residual vibration of the end-effector in view of the vibration acceleration. The settling time, namely the time interval between ∇ and ▼, is reduced down to about 1/2 (from 432 to 193ms) without the time-delay of the load's response.

4. INTEGRATION OF MODEL-BASED CONTROL INTO THE POSITION CONTROL LOOP

4.1 Construction of the position control loop

Fig.8 shows a block diagram of the model-base control system integrated into the position control loop. The P-action is used as a dynamical compensator of the position loop.

To set the proportional gain K_p of the P-action, the 3-mass system shown in Fig.1(b) is transformed into a concentrated mass system at the motor shaft. Further, the gain crossover frequency of the velocity control loop ω_{vc} is assumed to be much higher than that of the position control loop ω_{pc}. The transfer function of the velocity control loop is also assumed to be 1.0. Then, the position control loop can be regarded as a first order lag element. Finally, the relationship between K_p and ω_{pc} can be expressed as

$$K_p = \omega_{pc} . \quad (9)$$

Table 1. Simulation conditions.

Parameter			Value	Unit
Moment of inertia		J_m	1.362×10^{-5}	kg·m^2
		J_g	2.048×10^{-5}	
		J_l	2.852	
		J_l	1.205	
Torsional stiffness		K_s	889.6	N·m/rad
		K_g	6967.3	
Damping coefficient		C_s	0.0137	N·m·s/rad
		C_g	22.553	
Gear reducer Reduction ratio		R_g	100	−
Velocity loop gain		K_v	0.15	A/(rad/s)
Integral time constant		T_i	1.0	s
Torque constant		K_t	0.316	N·m/A
Voltage constant		K_e	0.316	V/(rad/s)
Phase resistance		R	4.5	Ω
Phase inductance		L	0.0189	H
Current loop gain		K_c	118.84	V/A
Current feedback gain		K_{cb}	1.0	−
Feedback gain		K_b	0 or -0.7	−
Reduced-order model				
Electrical part				
Natural frequency		ω_e	188.4	rad/s
		ζ_e	1.0	−
Mechanical part				
Natural	Posture1	ω_n	151.2	rad/s
	Posture2	ω_n	163.3	
Damping ratio		γ_n	0.7	−
Inertia	Posture1	R_n	8.363	−
	Posture2	R_n	3.256	

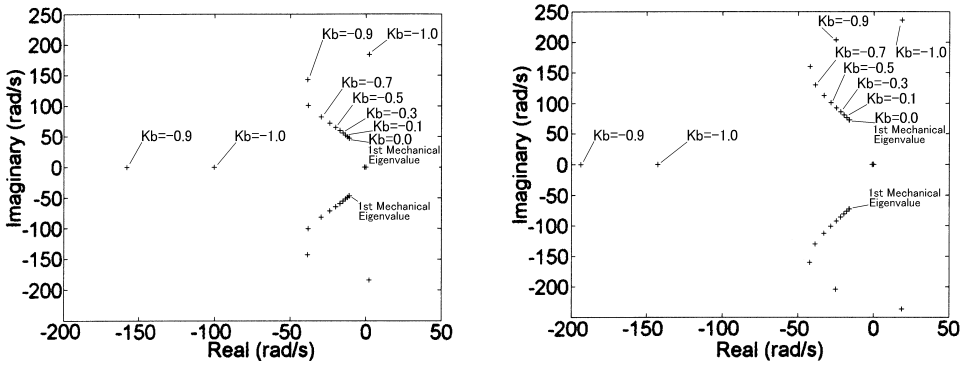

(a) In the case of Posture1 (N.F.=7Hz). (b) In the case of Posture2 (N.F.=12Hz).

Fig. 6. Loci of system eigenvalues.

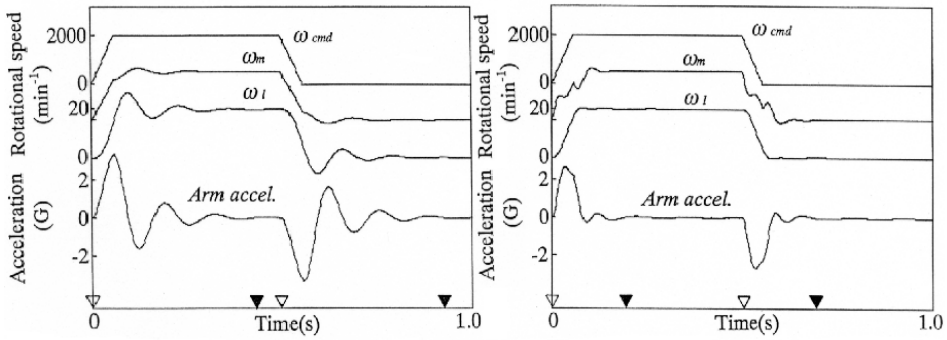

(a)Without model-based control. (b)With model-based control.

Fig. 7. Simulation results in the case of Posture1.

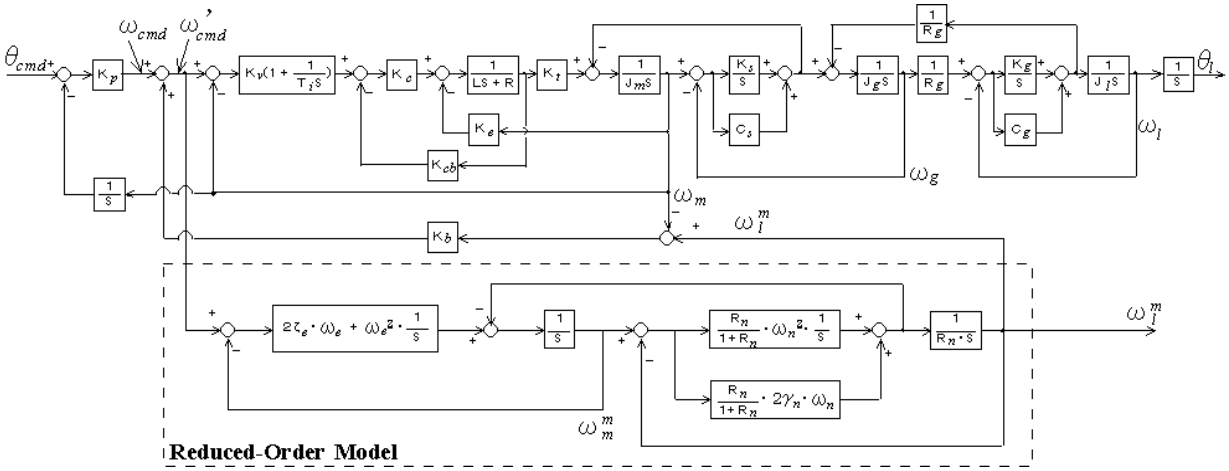

Fig. 8 Block diagram of the position control system with model-based control.

Besides, ω_{vc} can be written in Eq. (10) using K_v, K_t and J_t,

$$\omega_{vc} = \frac{K_v K_t}{J_t}, \tag{10}$$

where

$$J_t = J_m + J_g + J_l / R_g^2. \tag{11}$$

The relationship between ω_{vc} and ω_{pc} is expected to meet Eq. (12) to neglect the influence of the characteristic of the velocity control loop on that of the position control loop.

$$\omega_{pc} = K_p \le \frac{\omega_{vc}}{10}. \tag{12}$$

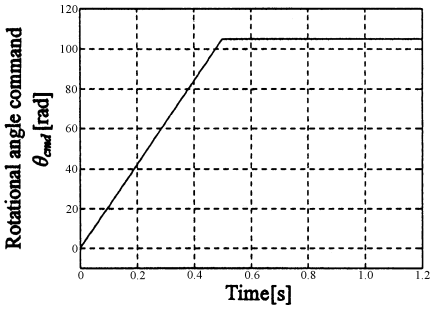

Fig. 9 Position command θ_{cmd}.

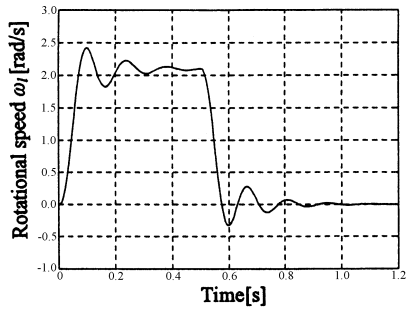

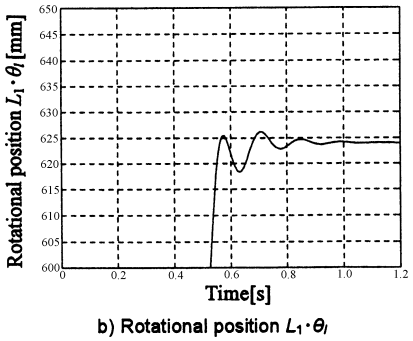

Fig. 10 Simulation results (Posture1, K_b=0.0)

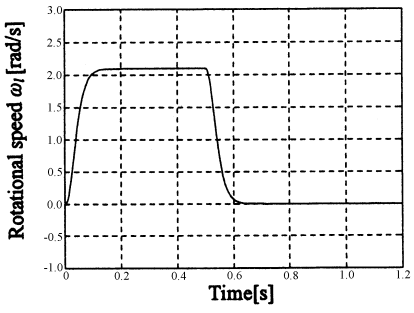

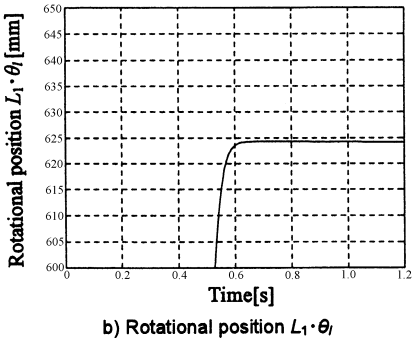

Fig. 11 Simulation results (Posture1, K_b= -0.7)

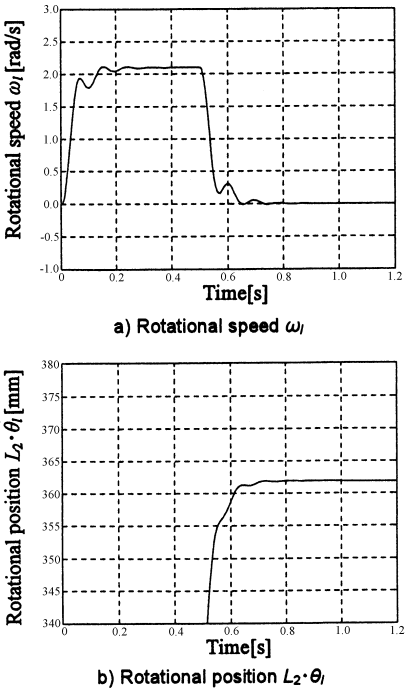

Fig. 12 Simulation results (Posture2, K_b=0.0)

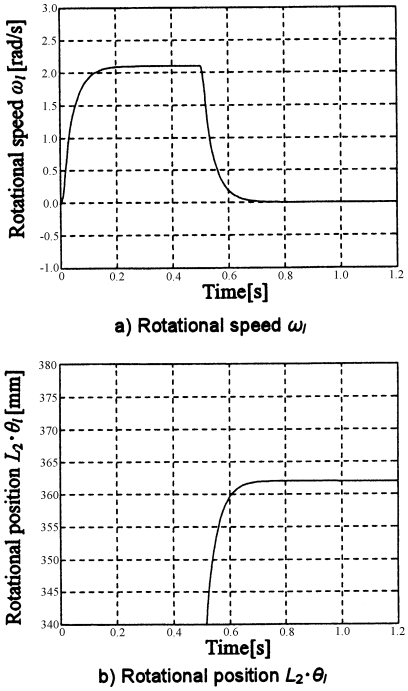

Fig. 13 Simulation results (Posture2, K_b= -0.7)

4.2 Simulation results on suppression of transient vibrations

To evaluate the suppression effects of the model-based control integrated into the position control loop, the articulated robot is regarded as a time-invariant system such that only the waist axis rotates.

Table 1 shows the simulation conditions. According to Eq. (12), K_p is set to 14.8rad/s as an allowable maximum value. The position command θ_{cmd} is shown in Fig.9. The total rotating angle of the end-effector is 60° (=1.047rad).

Fig.10 and Fig.11 show simulation results in the case of Posture1. The rotational speed ω_l of the end-effector and the rotational position $L_1 \cdot \theta_l$ of the arrival phase are shown in these figures. Here, θ_l represents angular rotation of the end-effector. In Fig.11, K_b is set to -0.7 according to the simulation results of the stability.

Making a comparison between Fig.10 and Fig.11, the transient vibration of 7Hz in the starting and arrival phases can be suppressed by using the model-based control.

Further, Fig.12 and Fig.13 show simulation results in the case of Posture2. In Fig.13, K_b is also set to -0.7. Making a comparison between Fig.12 and Fig.13, the transient vibration of 12Hz in the starting and arrival phases can be suppressed.

5. CONCLUSIONS

A model-based control was proposed as a technique of eliminating the transient vibration generated at the end-effector of the robot arm regarded as a time-invariant system. The control model is composed of electrical and mechanical parts related to the velocity control loop. The parameters of the control model can be obtained from design data or experimental data. In referring to the construction, this model-based control loop can be easily integrated into the position control loop as an inner loop.

The effectiveness of the model-based control integrated into the position control loop is verified by simulations. Simulations on the time responses show satisfactory control results in reducing the transient vibration of 7 Hz or 12 Hz which depends on the posture of the robot arm. As a result, the transient vibrations in the stating and the arrival phases of the operation can be suppressed.

REFERENCES

[1]Futami, S. et al., "Vibration Absorption Control of Industrial Robots by Acceleration Feedback," *IEEE Trans. Industrial Electronics*, vol. 30. No. 3, pp. 299-305, 1983.

[2]Yuki, K. et al., "Vibration Control of a 2-Mass Resonant System by the Resonance Ratio Control," *Trans. IEE Japan*, (in Japanese), vol.113(D), No. 10, pp.1162-1169, 1993.

[3]Honke, K. et al., "Motion and Vibration Control for Robot Arm with Elastic Joint (Application of Disturbance Observer Including Elastic Vibration)," *Trans. Jpn. Soc. Mech. Eng.*, (in Japanese), vol.60(C).No. 577, pp.3045-3050, 1994.

[4]Godler, I. et al., "Vibration Suppression for a Speed Control System with Gear," *J. Jpn. Soc. Prec. Eng.*, (in Japanese), vol.60.No.1, pp.86-90, 1994.

[5]Sakuta, H. et al., "Vibration Absorption Control of Robot Arm by Software Servomechanism (2nd Report)," *Trans. Jpn. Soc. Mech. Eng.*, (in Japanese), vol.54(C).No.497, pp.217-220, 1988.

[6]Itoh, M. et al., "Suppression of Transient Vibration for Geared Mechanical System (Effects of Model-based Control)," *Trans. Jpn. Soc. Mech. Eng.*, (in Japanese), vol.64(C).No.623, pp.2596-2601, 1998.

[7]Itoh, M. et al., "Vibration Suppression Control for an Articulated Robot: Effects of Model-Based Control Applied to a Waist Axis," *Proc. of ICCAS2001*, pp.176-181, 2001.

[8]Itoh, M. et al., "Vibration Suppression Control for an Articulated Robot: Effects of Model-Based Control Using Time-Varying Control Model," *Proc. of ICCAS2002*, pp.545-550, 2002.